Geometrical analysis of the opening gap after tibial condylar valgus osteotomy for proper hinge point selection

Xiaoyu Wang[#]^, Rui Zhang[#], Xu Zheng[#], Yifan Yu, Jia Xu, Qinglin Kang^

Department of Orthopedic Surgery, Shanghai Sixth People's Hospital Affiliated to Shanghai Jiao Tong University School of Medicine, Shanghai, China

Contributions: (I) Conception and design: X Wang, Q Kang; (II) Administrative support: Q Kang; (III) Provision of study materials or patients: X Wang, R Zhang, J Xu; (IV) Collection and assembly of data: X Wang, R Zhang, X Zheng, Y Yu; (V) Data analysis and interpretation: X Wang, R Zhang, X Zheng; (VI) Manuscript writing: All authors; (VII) Final approval of manuscript: All authors.

[#]These authors contributed equally to this work.

Correspondence to: Qinglin Kang, MD, PhD; Jia Xu, MD, PhD. Department of Orthopedic Surgery, Shanghai Sixth People's Hospital Affiliated to Shanghai Jiao Tong University School of Medicine, 600 Yishan Road, Shanghai 200233, China. Email: orthokang@163.com; xujia0117@126.com.

Background: Preoperative deformity and hinge position are associated with the magnitude of the gap opening during corrective osteotomy. A larger opening gap angle is associated with a higher risk of complications. This cross-sectional study sought to identify a suitable hinge position that results in the smallest opening angle during tibial condylar valgus osteotomy (TCVO).

Methods: The data of 66 arthritic knees treated by TCVO were included, comprising 16 knees with the hinge points selected medial to the center (group M), 21 knees with the hinge points selected at the center (group C), and 29 knees with the hinge points selected lateral to the center of the intercondylar eminence (group L). The opening gap angles and the correction amounts of the medial proximal tibial angle (*ΔMPTA*) were compared among the 3 groups to identify the preliminary relationship between the hinge positions and the opening gap angle. A simplified geometric model with the hinge positions selected at the medial beak, the center, and the lateral beak of the intercondylar eminence was constructed to simulate the realignment process. Several anatomical points were allocated as Cartesian coordinates. The opening gap angle with different hinge positions was mathematically formulated with MATLAB (MathWorks, Natick, MA, USA).

Results: The average *ΔMPTAs* were 9.4±2.9°, 9.4±3.5°, and 9.3±3.0° in groups L, C, and M, respectively. The opening angle of the osteotomy gap was the largest in group M and the smallest in group L (29.7±11.1° and 16.9±5.3°; P<0.01). The comparison of the opening angle per the *ΔMPTA* revealed a similar pattern. The simulated realignment process indicated that the hinge point at the lateral beak of the intercondylar eminence led to the smallest opening angle. The opening angle during TCVO was mathematically derived in terms of the *ΔMPTA*, the position of the intersection of the pre- and postoperative joint lines, and the position of the hinge point.

Conclusions: The hinge point at the lateral beak of the intercondylar eminence results in the smallest opening angle and may be suitable for TCVO.

Keywords: Tibial condylar valgus osteotomy (TCVO); opening gap; hinge position; medial proximal tibial angle; MATLAB

Submitted Apr 18, 2022. Accepted for publication Sep 13, 2022.
doi: 10.21037/atm-22-2022
View this article at: https://dx.doi.org/10.21037/atm-22-2022

^ ORCID: Xiaoyu Wang, 0000-0002-7276-9738; Qinglin Kang, 0000-0001-9825-0451.

Introduction

Opening-wedge high tibial osteotomy (OWHTO) is a standard prearthroplasty surgical method to treat arthritic knees with genu varum. It can restore joint function and reduce pain in the failing knee joint by realigning the weight-bearing axis (1,2). However, long-term follow-up studies have revealed several technical and clinical limitations of OWHTO in patients with intra-articular incongruency accompanied by lateral soft tissue laxity and a subluxated lateral joint (2-4). Tibial condylar valgus osteotomy (TCVO), a novel L-shaped osteotomy performed from the medial side of the proximal tibia to the intercondylar eminence, can adjust the congruity of the joint surface and improve intra-articular stability (5,6). TCVO has been reported to be an efficient technique for treating intra-articular deformity caused by degenerative arthritis (7,8), trauma (9), and growth disorders, such as Blount disease (5).

Preoperative deformity and hinge position are associated with the magnitude of the gap opening during the corrective osteotomy. A systematic review revealed an increased risk of lateral hinge fracture when the wedge is opened by >11 mm during OWHTO (10). The larger the magnitude of the opening gap is, the more medially aligned the medial portion of the proximal fragment and the more laterally aligned the medial portion of the distal fragment (11). A similar trend has been observed during TCVO, which is considered a special type of OWHTO (*Figure 1*). In such circumstances, a larger degree of mismatch between the patient-specific bony surface and the factory-made locking plate can impose a higher stress on the construct and weaken the structural stiffness of the implant, leading to an increased risk of technical complications, such as hinge fracture, screw pullout, and plate breakage (12-15). In addition, the significant prominence of the implant beneath the medial subcutaneous border and the small contact area between the plate and the bone at the distal end can cause postoperative pain (11,15). Thus, the hinge position that leads to the smallest gap opening angle should be favored by surgeons during TCVO.

Some recent studies have mentioned the hinge point as the lateral tip of the intercondylar eminence; however, no study has examined the exact reason for the selection of this point (5,6). To avoid iatrogenic injury to the joint surface of the tibial plateau during TCVO, the following 3 points were chosen for the candidate hinge position: (I) the hinge set at the medial beak, (II) the center, and (III) the lateral beak of the intercondylar eminence. Wang *et al.* showed that a larger gap opening angle was required in TCVO compared to OWHTO to correct the medial proximal tibial angle (MPTA) to the same extent (8). As TCVO can be regarded as a special form of OWHTO, with its hinge point positioned relatively medially, it was conjectured that the hinge position at the lateral part (i.e., the lateral beak of the intercondylar eminence) will result in a relatively smaller gap opening angle during TCVO (7,8). This study sought to (I) conduct retrospective evaluations of patients undergoing TCVO to identify the preliminary relationship between the magnitude of the opening gap and the hinge positions; (II) develop a simple and effective geometric model for surgical simulation and mathematical description; and (III) verify the hypothesis that among the 3 candidate hinge points, the hinge point at the lateral beak of the intercondylar eminence leads to the smallest gap opening angle after TCVO. We present the following article in accordance with the STROBE reporting checklist (available at https://atm.amegroups.com/article/view/10.21037/atm-22-2022/rc).

Methods

The study was conducted in accordance with the Declaration of Helsinki (as revised in 2013). The study was approved by ethics board of Shanghai Jiao Tong University affiliated Sixth People's Hospital (No. 2020-107), and informed consent was taken from all the patients. To identify the preliminary relationship between hinge positions and the magnitude of the opening gap, the data of patients with knee osteoarthritis (OA), genu varum, and intra-articular incongruency treated by TCVO at our institute from January 2015 to December 2021 were retrospectively reviewed. To be eligible for inclusion in this study, patients had to meet the following inclusion criteria: have symptomatic medial unicompartmental knee OA with varus malalignment (a femoral tibial angle over 182°), an intra-articular deformity (a "pagoda-type" tibial plateau, lateral joint dilation with a joint line convergence angle over 5°, and increased medial tibial plateau depression less than −4°), a range of flexion >90°, a flexion contracture <10°, and a near-normal lateral femorotibial compartment [defined in accordance with the magnetic resonance imaging for articular cartilage examination, the radiographic assessment for joint features, and a Kellgren-Lawrence (K-L) grade <2]. Patients were excluded from the study if they met any of the following exclusion criteria: had rheumatoid or

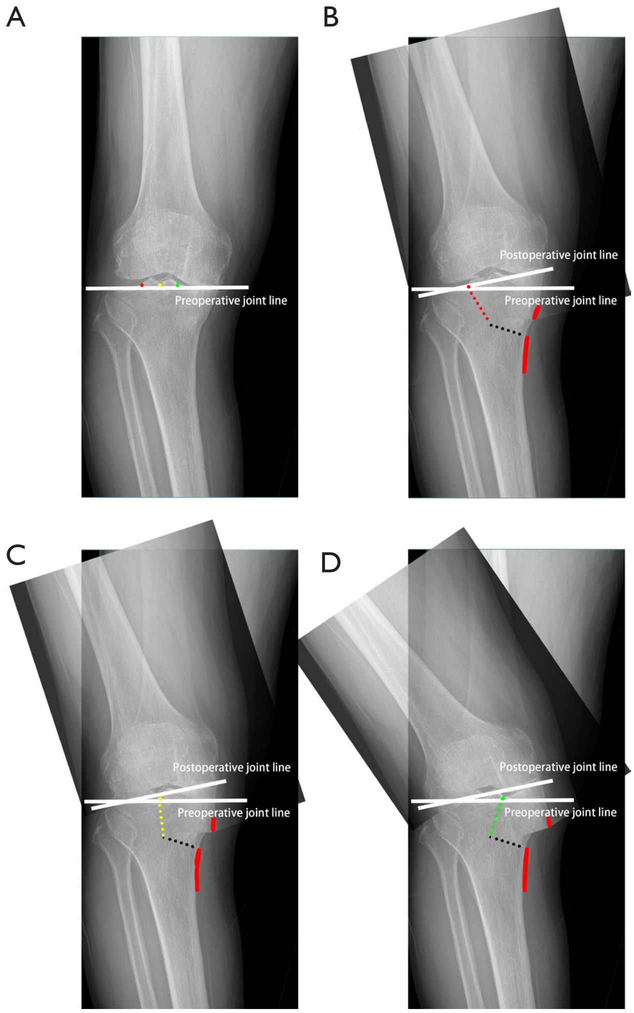

Figure 1 Geometric characteristics of the tibial plateau before and after TCVO. The lateral tibial plateau was set as a static reference object during the gap opening. For the surgical simulation, it was assumed that each surgery was performed at different hinge points [the dots are plotted in red, yellow, and green in (A)] to achieve the same ideal value of po-MPTA. Thus, the *ΔMPTA* was equal in each case. It should be noted that the larger degree of the opening gap was, the more medially aligned the medial portion of the proximal fragment and the more laterally aligned the medial portion of the distal fragment [the curve plotted in red in (B-D)]. TCVO, tibial condylar valgus osteotomy; MPTA, medial proximal tibial angle; po-MPTA, postoperative medial proximal tibial angle; *ΔMPTA*, correction amount of MPTA after each surgery.

inflammatory arthritis, advanced patellofemoral arthritis, or lateral unicompartmental knee OA (diagnosed by radiographic evidence and clinical manifestation); and were smokers. A total of 66 patients with OA knees were included in the study and divided into group M (comprising 16 knees with the hinge points selected medial to the center of the intercondylar eminence), group C (comprising 21 knees with the hinge points selected at the center of the intercondylar eminence), and group L (comprising 29 knees with the hinge points selected lateral to the center of the intercondylar eminence). The number of TCVO cases at our institute during the study period determined the sample size of the study. The K-L grading system was used to assess the grade of OA based on the evaluation of a standing posteroanterior radiograph (16). The demographic characteristics of the patients are set out in *Table 1*.

Anteroposterior long-leg weight-bearing radiographs were collected to measure and compare the correction amount of MPTA (*ΔMPTA*) between the 3 groups. MPTA was defined as the angle formed between the tibial mechanical axis and the joint surface of the proximal tibia. The percentage of mechanical axis (%MA) was defined as the point at which the tibial plateau intersects the mechanical axis, converted to a percentage from the medial edge (0%) to the lateral edge (100%) of the tibial plateau. For each case, the ideal postoperative MPTA (po-MPTA) aimed to achieve a weight-bearing line with 60% %MA.

The opening angle refers to the angle formed between 2 osteotomy lines after opening the osteotomy gap. The opening angle was measured by a ruler and confirmed by plotting the opening wedge on the intra-operative radiograph during the gap opening (*Figure 2*). The preoperative evaluations and all the operations were performed by 2 surgeons. Surgical indications and details of the TCVO procedures were similar to those described previously (5,6). Radiographic measurements were recorded twice by 2 independent observers at an interval of 6 weeks. The examiners were blinded to each other's results. The intra- and interrater reliability of the measurements were assessed by examining the intraclass correlation coefficients.

For the geometrical analysis of the opening gap, schematic figures were generated to perform the simulation. The following procedure was adopted:

(I) preoperative MPTA (pre-MPTA) and po-MPTA were defined as the medial proximal tibial angle before and after the surgery, respectively. *ΔMPTA* was defined as follows:

$$\Delta MPTA = po\text{-}MPTA - pre\text{-}MPTA \quad [1]$$

For the surgical simulation, it was assumed that each surgery was performed with different

Table 1 Patients' demographic characteristics

Demographic indicators	Group M	Group C	Group L
Knees (male/female), n	16 (8/8)	21 (9/12)	29 (13/16)
Age (years), mean [range]	59 [45–77]	61 [42–75]	57 [40–76]
BMI (kg/m^2), mean [range]	26.1 [21.9–28.6]	26.4 [21.5–28.6]	25.8 [21.1–28.1]
K-L grade (II, III, IV), n	1, 9, 6	2, 12, 7	3, 16, 10

Group M, the knees with the hinge points selected medial to the center of the intercondylar eminence; group C, the knees with the hinge points selected at the center of the intercondylar eminence; group L, the knees with the hinge points selected lateral to the center of the intercondylar eminence; BMI, body mass index; K-L, Kellgren-Lawrence.

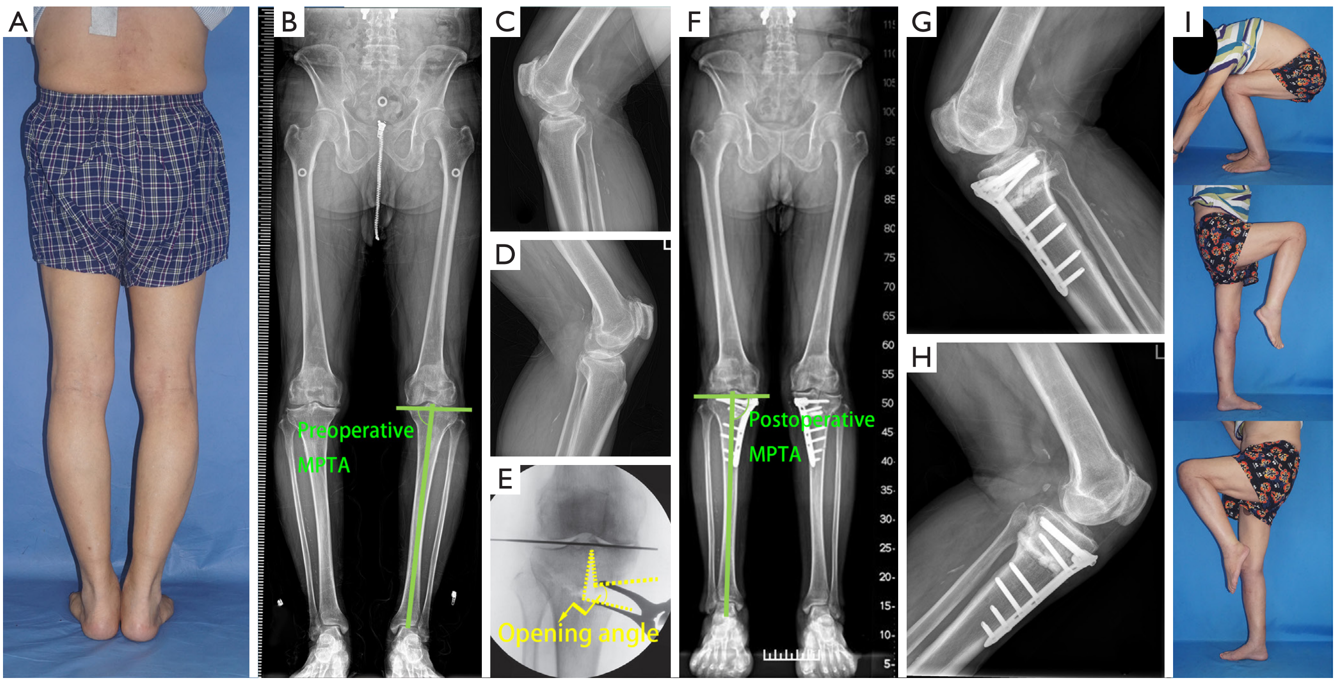

Figure 2 A typical case of TCVO with the hinge point selected at the lateral beak of the intercondylar eminence. Preoperative appearance (A) and standing radiograph (B) of the lower extremities. Preoperative lateral radiographs of the right (C) and the left (D) knee joints. Fluoroscopic intraoperative view of the knee undergoing TCVO (E). The angle formed between the margins of the osteotomy gap was defined as the opening angle. Postoperative standing radiograph of the lower extremities after surgery (F). Postoperative lateral radiographs of the right (G) and the left (H) knee joints after surgery. The patient was able to squat and jog after TCVO (I). This image was published with the patient's consent. TCVO, tibial condylar valgus osteotomy; po-MPTA, postoperative medial proximal tibial angle; pre-MPTA, preoperative medial proximal tibial angle.

hinge points to achieve the same ideal value of po-MPTA. Thus, the *ΔMPTA* was equal for each of the references (the hinge set at the lateral beak, the center, and the medial beak of the intercondylar eminence; *Figure 1*).

(II) Adobe Illustrator (Adobe Inc., Mountain View, CA, USA) was used to construct the schematic figures (*Figure 3*). The preoperative joint line was the projected tangent to the lowest points of the tibial plateau both at the medial and lateral sides. The lateral tibial plateau was set as a static reference object in this model. Thus, during TCVO, the medial tibial plateau was rotated around the selected hinge point until the medial tibial plateau was

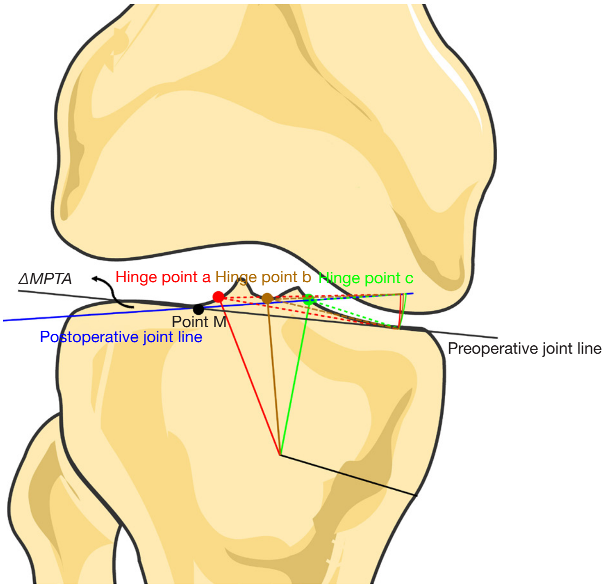

Figure 3 2D schematic model of genu varum correction. The preoperative joint line was projected tangentially to the lowest points of the tibial plateau at the medial and lateral sides before TCVO. The postoperative joint line should be tangential to the lowest point of the lateral tibial plateau, with the angle formed between the pre- and postoperative joint lines equal to *ΔMPTA*. TCVO, tibial condylar valgus osteotomy; MPTA, medial proximal tibial angle; *ΔMPTA*, correction amount of MPTA after each surgery; point M, the intersection of the pre- and postoperative joint lines that located medial to the point at which the joint line was tangential to the lateral tibial plateau.

tangential to the ideal postoperative joint line and the ideal *ΔMPTA* was achieved. The postoperative joint line was thus projected tangentially to the lowest point of the static lateral tibial plateau, with the angle formed between the pre- and postoperative joint lines equal to the *ΔMPTA*. Point *M*, which was defined as the intersection point of the pre- and postoperative joint lines, was located medially to the point at which the preoperative joint line was tangential to the lateral tibial plateau. To define the hinge point, a marking line (hinge line) was drawn, running from the medial beak of the intercondylar eminence (point *c*), passing through the center of the intercondylar eminence (point *b*), and ending at the lateral beak of the intercondylar eminence (point *a*).

(III) For the preliminary analysis of the simulated realignment process at the coronal plane, the preoperative joint line was set to pass through the selected 3 hinge points, as the distance of these hinge points to the preoperative joint line was negligible compared to the distance between these 3 hinge points. The simulated gap opening procedure was performed by rotating the medial tibial plateau and distal femur around the selected hinge point until the lowest point of the medial tibial plateau became tangential to the postoperative joint line (*Figure 4*). The opening angle α subtended lines from the hinge points to the medial margin of the tibia on the preoperative joint lines and hinge points to this medial margin of the tibia after simulation.

Several anatomical points on the schematic figure were allocated as Cartesian coordinates in a theoretical layer over the radiograph (*Figure 5*). The joint line intersection point *M* was assigned as the origin of the coordinate system. The preoperative joint line that paralleled the hinge line was set as the vector on the *X*-axis with the positive *X* direction corresponding to the lateral-to-medial limb direction. The coordinate information was set according to the measurement of the dimensions of the proximal tibia performed based on the anteroposterior radiograph from *Figure 1*. The horizontal width of the tibial plateau was set as 1 unit. The hinge points on the hinge line were placed horizontally. The vertical distance between the hinge line and preoperative joint line was 0.05 units in length. The horizontal distances between each hinge point were X_{ab} = X_{bc} =0.20 units in length, respectively. Point *d* was set as the medial point of the tibial plateau on the preoperative joint line. The horizontal distance between point *d* and hinge point *a* was X_{ad} =0.625 units in length, and this value conformed with the position of the Fujisawa's point (17). As the osteotomy gap can be increased gradually until the desired *ΔMPTA* is achieved, point *M* moves along the preoperative joint line toward the medial side. According to the measurement shown in *Figure 1*, the distance between point *M* and point *a* was designated as 0.1 to 0.375 units in length (*Figure 5*). The mathematical calculation of the opening angle (α_a, α_b, and α_c, respectively) was performed by MATLAB (MathWorks, Natick, MA, USA) R2020b using the following variables: (I) the correction angle *ΔMPTA*; and (II) *Xp*, which was defined as the horizontal distance between point *M* and each candidate hinge point *a*, *b*, and *c*. Surgical simulations of geometrical models with different

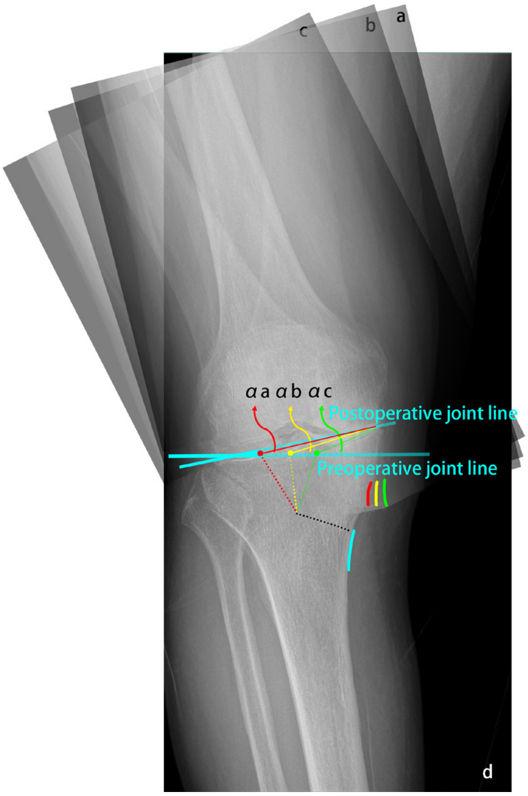

Figure 4 Simulation of the realignment process at the coronal plane achieved by rotating the medial tibial plateau and distal femur around the selected hinge point until the medial tibial plateau was tangential to the postoperative joint line. The opening angle, α, was annotated with the apex at the selected hinge points. This angle subtended lines from the hinge point to the medial margin of the tibia on preoperative joint lines and the hinge point to this medial margin of the tibia after simulation. It should be noted that the larger magnitude of the opening gap was, the more medially aligned the medial cortical line of the proximal tibia (the curves are plotted in red, yellow, and green along the medial cortical line).

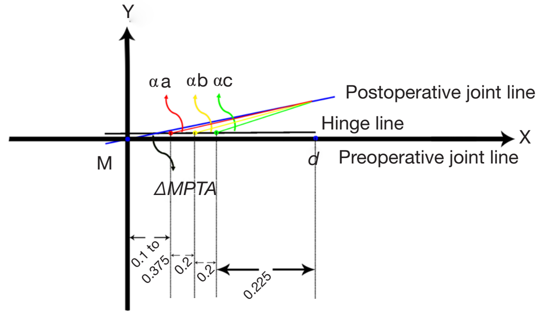

Figure 5 Anatomical points on the schematic figure. The horizontal width of the tibial plateau was set as 1 unit in length. The vertical distance between the hinge line and preoperative joint line was 0.05 units in length. The horizontal distances between hinge points were X_{ab} = X_{bc} =0.20 units in length, respectively. Point *d* was set as the most medial point of the tibial plateau on the preoperative joint line. The joint line intersection point *M* was assigned as the origin of the coordinate system. Point *M* moves from the lateral margin of the tibial plateau (when *ΔMPTA* approaches 0°) to the point at a distance of 10% of the length of the tibial plateau away from the hinge point *a* (when *ΔMPTA* reaches the largest value, which is 35°, under the clinical scenario). Thus, the distance between point *M* and hinge point *a* was 0.1 to 0.375 units in length. The horizontal distance between point *d* and hinge point *a* was X_{ad} =0.625 units in length. *ΔMPTA*, the correction amount of MPTA after each surgery.

values of *ΔMPTA* from 5° to 35° in increments of 3.333° were conducted (For further details of the code, see the Appendix 1).

Statistical analysis

SPSS Statistics version 23 was used for the statistical analysis. The data were evaluated for normality using the Shapiro-Wilk test. Statistical differences between the 3 groups were evaluated using an analysis of variance test for the continuous variables with a normal distribution and a Kruskal-Wallis test for the continuous variables with a nonnormal distribution. Results with a 2-tailed P value <0.05 were considered statistically significant.

Results

The demographic characteristics did not differ significantly among the 3 groups (*Table 1*). The inter- and intrarater reliabilities were satisfactory for the parameters, including the *ΔMPTA* (0.96 and 0.97) and the opening angle (0.96 and 0.97). No significant difference was observed in terms of the average *ΔMPTA* among the 3 groups (9.4±2.9°, 9.4±3.5°, and 9.3±3.0° for groups L, C, and M, respectively). The opening angle of the osteotomy gap differed significantly among the 3 groups (P<0.01), with the largest value in group M (29.7±11.1°) and the smallest value in group L (16.9±5.3°). A comparison of the opening angles per

Table 2 The correction amount of MPTA and the gap-opening angle in groups L, C, and M

Items	Group M	Group C	Group L	P value
ΔMPTA (°)	9.3±3.0	9.4±3.5	9.4±2.9	n.s.
Opening angle (°)	29.7±11.1	20.6±7.2	16.9±5.3	<0.01
Opening angle per *ΔMPTA*	3.2±0.5	2.2±0.2	1.8±0.2	<0.01

Data are shown as mean ± SD. *ΔMPTA*, the correction amount of MPTA after each surgery; *ΔMPTA* = post-MPTA − pre-MPTA; opening angle, the angle formed between 2 osteotomy lines after osteotomy gap opening; opening angle per *ΔMPTA* = opening angle/*ΔMPTA*; n.s., nonsignificant; group M, the knees with the hinge points selected medial to the center of the intercondylar eminence; group C, the knees with the hinge points selected at the center of the intercondylar eminence; group L, the knees with the hinge points selected lateral to the center of the intercondylar eminence.

the *ΔMPTA* revealed a similar pattern, with significant differences across the 3 groups (P<0.01; *Table 2*).

Development of a simple and effective geometric model for surgical simulation and mathematical description

A 2-dimensional (2D) schematic model of genu varum is shown in *Figure 3*, and the simulated realignment process at the coronal plane is shown in *Figure 4*. The opening angle with the hinge point at the lateral beak of the intercondylar eminence (α_a) was the smallest, while the gap opening angle with the hinge point at the medial beak of the intercondylar eminence (α_c) was the largest.

Quantitative verification of the hypothesis that the hinge point at the lateral beak of the intercondylar eminence leads to the smallest gap opening angle

Mathematical equations for predicting the opening angle α_a, α_b, and α_c (°), with different hinge points *a*, *b*, and *c* selected, were calculated by MATLAB R2020b. The detailed formulae are provided as follows:

$$\alpha_a = \frac{180}{\pi} \times \arccos\left(\frac{50\times k - 80\times X_p \times k - 1000\times X_p \times k^2 - (2\times k - 25)\times\sqrt{-1600\times X_p^2\times k^2 + 160\times X_p\times k + 629\times k^2 + 625} + 4}{629\times(k^2+1)}\right) \quad [2]$$

$$\alpha_b = \frac{180}{\pi} \times \arccos\left(\frac{34\times k - 80\times X_p \times k - 680\times X_p \times k^2 - (2\times k - 17)\times\sqrt{-1600\times X_p^2\times k^2 + 160\times X_p\times k + 293\times k^2 + 289} + 4}{293\times(k^2+1)}\right) \quad [3]$$

$$\alpha_c = \frac{180}{\pi} \times \arccos\left(\frac{18\times k - 80\times X_p \times k - 360\times X_p \times k^2 - (2\times k - 9)\times\sqrt{-1600\times X_p^2\times k^2 + 160\times X_p\times k + 85\times k^2 + 81} + 4}{85\times(k^2+1)}\right) \quad [4]$$

The variable *k* was defined as follows: *k = tan (ΔMPTA)*.

The variable *Xp* was defined as the horizontal distance between point *M* and the selected hinge points *a*, *b*, and *c*.

The mathematical relationship between the opening angle and the location of the hinge point is shown in *Figure 6*. *Xp* ranged from 0.1 to 0.375 units in length when hinge point *a* was selected, from 0.3 to 0.575 units in length when hinge point *b* was selected, and from 0.5 to 0.775 units in length when hinge point *c* was selected. As the *ΔMPTA* increased gradually from 5° to 35° in increments of 3.333°, the opening angle of the bony fragment increased correspondingly. In relation to the opening angle required with a certain value of the *ΔMPTA*, the function image suggested that the opening angle with the hinge at the lateral beak of the intercondylar eminence (the curve plotted in red) was always the smallest, while the opening angle with the hinge at the medial beak of the intercondylar eminence (the curve plotted in green) was always the largest. It should be noted that the TCVO procedure with the hinge at the medial beak of the intercondylar eminence had limited capacity to achieve a satisfying correction angle. As shown by the curve plotted in green, the largest value

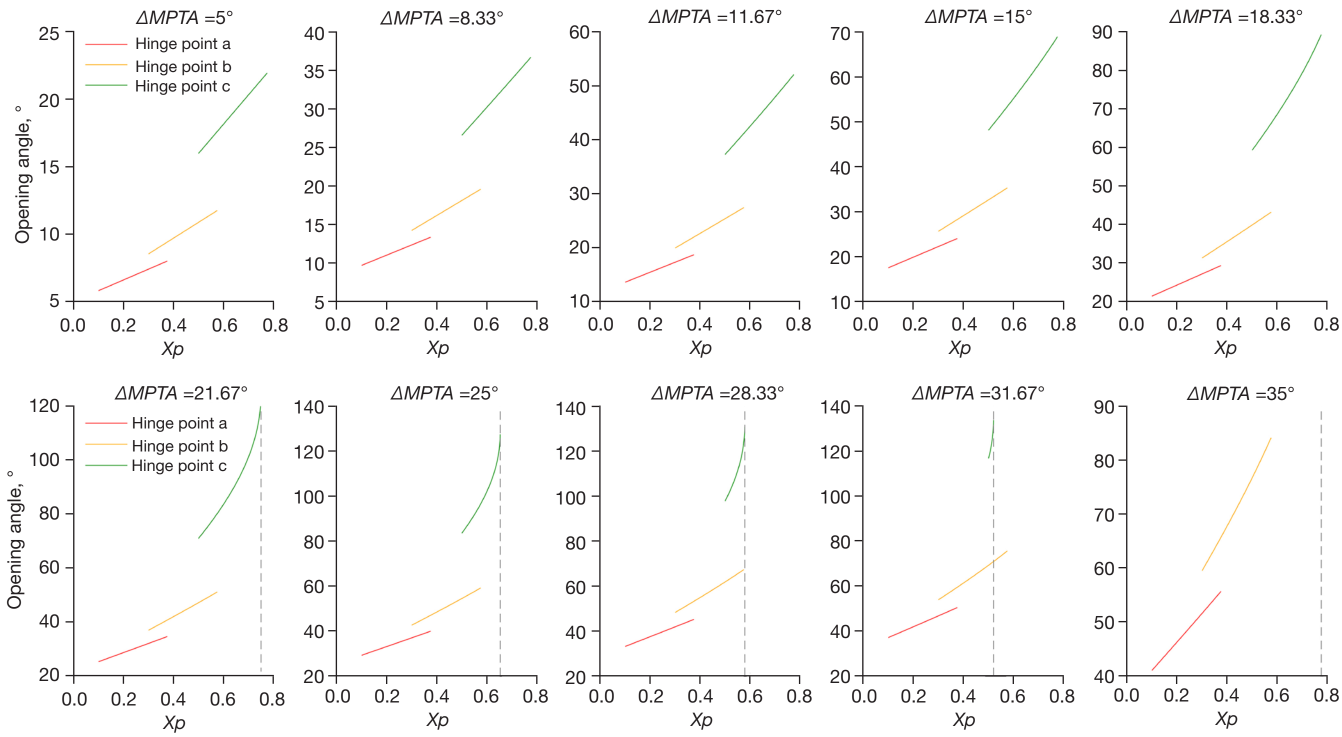

Figure 6 Function curves explaining the relationship between the opening angle and the hinge position. *Xp* ranged from 0.1 to 0.375, from 0.3 to 0.575, and from 0.5 to 0.775 units in length for hinge points *a*, *b*, and *c*, respectively. Under a certain value of *ΔMPTA*, the opening angle with the hinge at the lateral beak of the intercondylar eminence (the curve plotted in red) was always the lowest, while the opening angle with the hinge at the medial beak of the intercondylar eminence (the curve plotted in green) was always the largest. *Xp*, the horizontal distance between point *M* and each candidate hinge point *a*, *b*, and *c*; *ΔMPTA*, the correction amount of MPTA after each surgery.

of the opening angle approached infinity, and no value of the opening angle could be determined when a large scale of the *ΔMPTA* (28.33°, 31.67°, and 35°) was required. (For further details of the MATLAB code, see the Appendix 1).

Discussion

The most important finding of the present study was that preoperative deformity and the hinge position correlated with the degree of gap opening during TCVO. Additionally, the opening angle with the hinge point at the lateral beak of the intercondylar eminence was the lowest compared to the hinge point at the center or the medial beak of the intercondylar eminence.

Importance of choosing the hinge point at the lateral part of the tibial plateau that results in a relatively small opening angle during TCVO

With the gradual opening of the osteotomy gap, the horizontal distance between the proximal fragments, distal fragments, and the bone-plate clearance increase correspondingly (11,12,15). A bone-plate mismatch may increase the risk of implant failure from, for example, locking pin backout or screw breakage after tibial osteotomy (18-20). Screws and bone plates must bear a large mechanical load to support the "artificially caused" fracture fixation. An appropriate hinge position with the smallest opening gap ensures adequate structural stability, which is essential for minimizing the risk of nonunion and maintaining the corrected alignment, especially when encouraging early weight-bearing that will benefit bone healing at the osteotomy site. A recent study revealed that TCVO required a larger gap opening magnitude than did OWHTO when MPTA was corrected to the same extent. Thus, OWHTO has more advantages in angle correction, but this capacity is limited in TCVO (8). Kuwashima *et al.* also demonstrated that compared to OWHTO, TCVO requires more degrees of gap opening for angle correction (5). As TCVO can be regarded as a special form of OWHTO, with hinge point positioned more medially than in OWHTO, it was speculated that selecting the lateral part for the hinge point would lead to a relatively small opening angle when raising the gap.

Development of a simple and effective geometric model for surgical simulation and mathematical description

To gather evidence supporting this hypothesis, surgical simulations with clear mathematical expressions were considered appropriate. Improvements in image identification technology together with the incorporation of computer navigation, 3-dimensional (3D) visualized simulation, and the use of other technical advances have increased the applicability of OWHTO and enabled accurate preoperative planning and better outcome predictability (21-23). However, almost no research into the related field of TCVO has been conducted, nor has any research been conducted on the definite selection of the hinge position and its relationship to the magnitude of the gap opening during this procedure. This may be due to the lack of a simple and effective preoperative planning model. Paley *et al.* described basic concepts of the deformity analysis which included the following 3 key questions (24): (I) Does the patient present a bony deformity? (II) Where is the center of rotation angulation (CORA)? (III) What is the degree of the corrective angle?

Anatomical or mechanical axes have been applied in various preoperative planning methods for OWHTO (25). Based on these methods and principles, a geometrical model with a particular focus on the hinge position and correction angle (the change in MPTA) was developed in this study. This geometrical model with pre- and postoperative tibial joint lines is advantageous, as the surgeon can outline a moving trace of the osteotomized bony fragments until alignment is satisfactory while observing intra-articular incongruency. This model also conforms to Paley's principles in terms of deformity correction (24). Similarly, a different geometrical model with the same principle could be employed when planning a DFOTO procedure (distal femoral osteotomy associated with the isolated TCVO) or a DLOTO procedure (double-level osteotomy associated with TCVO), but this was not investigated in this study.

Quantitative verification of the hypothesis that the hinge point at the lateral beak of the intercondylar eminence will lead to the smallest gap opening angle

The surgical realignment simulation supported the preliminary hypothesis. The quantified results for the geometrical calculation of the opening gap with 3 different hinge positions under allocated Cartesian coordinates are encouraging. Through MATLAB programming, mathematical equations with parameterized geometrical factors of TCVO were successfully derived. The hypothesis that the hinge point at the lateral beak of the intercondylar eminence leads to the lowest opening angle during TCVO was thus confirmed. The accurate identification of indications and a detailed surgical plan ensure effective correction and proper alignment. The adage "measure with a microscope, mark with chalk, and cut with an axe" describes the crucial role of attempting to ensure accuracy during OWHTO (25). This is also true in the context of TCVO.

Additional procedures may be essential for cases with large opening gaps

Due to the challenge of unfavorable structural conditions of open-wedge osteotomy, complications, such as loss of correction, hinge fracture, and hardware failure, are common, especially for cases with large correction angles (10,18,19). Chieh-Szu Yang *et al.* introduced the additional insertion of a pretensioned opposite lag screw from the lateral cortex upward to the region beneath the medial plateau at an orientation of approximately 38.5° oblique to the transverse plane and 50° oblique to the coronal plane to improve the structural stability by providing an internally stiffer support against the outer physiological loads in OWHTO. A biomechanical evaluation of the finite element model provided evidence of its utility in preventing the aforementioned complications (20). A similar procedure with the opposite screw inserted may serve as a protective strategy for patients undergoing TCVO with large correction angles. Obviously, positioning the hinge point relatively laterally on the tibial plateau increases the contact area between the opposite screw and the region beneath the medial plateau, which can provide a greater pretension force from the lag screw and share the partial mechanical load from the conventional assignment of the locking screws and bone plate.

The proper fitting of the plate to the bony surface is essential for the appropriate and effective delivery of physiological stress, which prevents a loss of fixation stability and plate fracture (13-15,26). Previous biomechanical studies have also revealed that a large clearance between the locking plate and the bone beneath the plate is associated with a greater concentration of stress at the construct, increased pressure at the lateral hinge, and weakened axial stiffness (27-29). It has been recommended that bone-plate clearance be kept at a distance of no more than 5 mm to maintain the regional periosteal blood supply and allow a mechanically stable environment for fracture healing (29). Solomin *et al.* performed OWHTO simulations on the genu varum with different values of MPTA (from 40° to 85°) and found that in the cases with a preoperative MPTA ≤70°, the distance between the lower edge of the fixation plate and the medial surface of the tibia exceeded 11 mm, resulting in unacceptable soft-tissue tension around the plate (12). Yoo *et al.* conducted a 3D analysis to investigate 69 cases of OWHTO and found that after OWHTO, the surface curvature of the medial bony contour line at the coronal plane tended to decrease from the proximal to the distal direction (11). According to Paley's concept, for severe genu varum with intra-articular deformity, the performance of a corrective osteotomy at the level away from CORA requires the transverse movement of the distal bony fragment to align the proximal and distal axes of the relevant bone segments (24). As more gap-opening degrees are required for an angle correction than for OWHTO, the anatomy of the medial aspect of the proximal tibia undergoing TCVO displays the same pattern, but to a greater degree (5,8).

The patient- and TCVO-specific features at the osteotomy site made it difficult to fit a factory-made locking plate with tibial geometry, and a large bone-plate clearance is unavoidable, especially when the *ΔMPTA* is large. To address this issue, intraoperative plate contouring at both ends of the opening gap may help to fit the surface geometry. However, the accuracy of this technique is rather low and requires the surgeon to be proficient (15). The application of the circular external fixator or additional fixation on the more medial aspect of the tibia would be necessary but would increase the surgical difficulty and costs (11,30). Customized and patient-specific implants fabricated by a 3D-printing technique might ensure satisfactory contouring, but this method is often criticized for its high costs and low fatigue strength (15,31). Unlike the incomplete osteotomy of OWHTO, which has an intact lateral cortex for supporting the construct after surgery, TCVO can be regarded as a complete osteotomy with a proximal tibial fracture. Thus, further research is needed to develop a fixation technique that meets the strict requirements of construct stability in TCVO.

Limitations

This study had several limitations. First, it was conducted via a retrospective investigation and innovative geometrical analysis. Thus, clinical trials need to be conducted to confirm the clinical significance of our observations. Second, the models were only studied under static and normal conditions. The dynamic moving track of the osteotomized bony fragments under complex loading conditions in each spatial plane requires further study. Third, the biomechanical performance of TCVO under 3 different conditions should be examined. Further research needs to be conducted to provide a virtual biomechanical evaluation of different hinge positions during TCVO.

Conclusions

This study showed that the hinge point at the lateral margin of the intercondylar eminence led to the smallest gap-opening angle during TCVO. The relationship between the magnitude of the gap opening and different hinge points, as determined by this retrospective clinical study, simulated geometric model, and mathematic analysis provides a deeper understanding of hinge point selection during TCVO.

Acknowledgments

Funding: This work was supported by the National Natural Science Foundation of China (grant Nos. NSFC 81802156 and 82072421).

Footnote

Reporting Checklist: The authors have completed the STROBE reporting checklist. Available at https://atm.amegroups.com/article/view/10.21037/atm-22-2022/rc

Data Sharing Statement: Available at https://atm.amegroups.com/article/view/10.21037/atm-22-2022/dss

Peer Review File: Available at https://atm.amegroups.com/article/view/10.21037/atm-22-2022/prf

Conflicts of Interest: All authors have completed the ICMJE uniform disclosure form (available at https://atm.amegroups.com/article/view/10.21037/atm-22-2022/coif). The authors have no conflicts of interest to declare.

Ethical Statement: The authors are accountable for all aspects of the work in ensuring that questions related to the accuracy or integrity of any part of the work are appropriately investigated and resolved. The study was conducted in accordance with the Declaration of Helsinki (as revised in 2013). The study was approved by ethics board of Shanghai Jiao Tong University Affiliated Sixth People's Hospital (No. 2020-107), and informed consent was taken from all the patients.

References

1. Brinkman JM, Lobenhoffer P, Agneskirchner JD, et al. Osteotomies around the knee: patient selection, stability of fixation and bone healing in high tibial osteotomies. J Bone Joint Surg Br 2008;90:1548-57.
2. Duivenvoorden T, Brouwer RW, Baan A, et al. Comparison of closing-wedge and opening-wedge high tibial osteotomy for medial compartment osteoarthritis of the knee: a randomized controlled trial with a six-year follow-up. J Bone Joint Surg Am 2014;96:1425-32.
3. Giuseffi SA, Replogle WH, Shelton WR. Opening-Wedge High Tibial Osteotomy: Review of 100 Consecutive Cases. Arthroscopy 2015;31:2128-37.
4. Akamatsu Y, Ohno S, Kobayashi H, et al. Coronal subluxation of the proximal tibia relative to the distal femur after opening wedge high tibial osteotomy. Knee 2017;24:70-5.
5. Kuwashima U, Yonekura A, Itoh M, et al. Tibial condylar valgus osteotomy - indications and technique. J Exp Orthop 2020;7:30.
6. Higuchi T, Koseki H, Yonekura A, et al. Comparison of radiological features of high tibial osteotomy and tibial condylar valgus osteotomy. BMC Musculoskelet Disord 2019;20:409.
7. Chiba K, Yonekura A, Miyamoto T, et al. Tibial condylar valgus osteotomy (TCVO) for osteoarthritis of the knee: 5-year clinical and radiological results. Arch Orthop Trauma Surg 2017;137:303-10.
8. Wang X, Shi L, Zhang R, et al. Salvage of severe knee osteoarthritis: efficacy of tibial condylar valgus osteotomy versus open wedge high tibial osteotomy. J Orthop Surg Res 2021;16:451.
9. Watanabe Y, Takenaka N, Kinugasa K, et al. Intra- and Extra-Articular Deformity of Lower Limb: Tibial Condylar Valgus Osteotomy (TCVO) and Distal Tibial Oblique Osteotomy (DTOO) for Reconstruction of Joint Congruency. Adv Orthop 2019;2019:8605674.
10. Kim JH, Lee DK, Park YB. Computed Tomography Detects Hinge Fractures After Medial Opening Wedge High Tibial Osteotomy: A Systematic Review. Arthroscopy 2021;37:1337-52.
11. Yoo OS, Lee YS, Lee MC, et al. Morphologic analysis of the proximal tibia after open wedge high tibial osteotomy for proper plate fitting. BMC Musculoskelet Disord 2016;17:423.
12. Solomin LN, Chugaev DV, Filippova AV, et al. High Tibial Osteotomy for Genu Varum in Adults: Do Proprietary Implants Limit the Quality of Correction? Strategies Trauma Limb Reconstr 2020;15:13-22.
13. Nelissen EM, van Langelaan EJ, Nelissen RG. Stability of medial opening wedge high tibial osteotomy: a failure analysis. Int Orthop 2010;34:217-23.
14. Luo CA, Lin SC, Hwa SY, et al. Biomechanical effects of plate area and locking screw on medial open tibial osteotomy. Comput Methods Biomech Biomed Engin 2015;18:1263-71.
15. Hayatbakhsh Z, Farahmand F. Effects of plate contouring quality on the biomechanical performance of high tibial osteotomy fixation: A parametric finite element study. Proc Inst Mech Eng H 2022;236:356-66.
16. KELLGREN JH, LAWRENCE JS. Radiological assessment of osteo-arthrosis. Ann Rheum Dis 1957;16:494-502.
17. Fujisawa Y, Masuhara K, Shiomi S. The effect of high tibial osteotomy on osteoarthritis of the knee. An arthroscopic study of 54 knee joints. Orthop Clin North Am 1979;10:585-608.

18. Otsuki S, Murakami T, Morikura R, et al. Back out of Locking Pin with Hinge Fracture after High Tibial Osteotomy. Knee Surg Relat Res 2018;30:171-5.
19. Chae DJ, Shetty GM, Wang KH, et al. Early complications of medial opening wedge high tibial osteotomy using autologous tricortical iliac bone graft and T-plate fixation. Knee 2011;18:278-84.
20. Chieh-Szu Yang J, Chen CF, Lee OK. Benefits of opposite screw insertion technique in medial open-wedge high tibial osteotomy: A virtual biomechanical study. J Orthop Translat 2020;20:31-6.
21. Specogna AV, Birmingham TB, DaSilva JJ, et al. Reliability of lower limb frontal plane alignment measurements using plain radiographs and digitized images. J Knee Surg 2004;17:203-10.
22. Sled EA, Sheehy LM, Felson DT, et al. Reliability of lower limb alignment measures using an established landmark-based method with a customized computer software program. Rheumatol Int 2011;31:71-7.
23. Schröter S, Ihle C, Mueller J, et al. Digital planning of high tibial osteotomy. Interrater reliability by using two different software. Knee Surg Sports Traumatol Arthrosc 2013;21:189-96.
24. Paley D, Herzenberg JE, Tetsworth K, et al. Deformity planning for frontal and sagittal plane corrective osteotomies. Orthop Clin North Am 1994;25:425-65.
25. Elson DW, Petheram TG, Dawson MJ. High reliability in digital planning of medial opening wedge high tibial osteotomy, using Miniaci's method. Knee Surg Sports Traumatol Arthrosc 2015;23:2041-8.
26. Takeuchi R, Woon-Hwa J, Ishikawa H, et al. Primary stability of different plate positions and the role of bone substitute in open wedge high tibial osteotomy. Knee 2017;24:1299-306.
27. Bottlang M, Doornink J, Fitzpatrick DC, et al. Far cortical locking can reduce stiffness of locked plating constructs while retaining construct strength. J Bone Joint Surg Am 2009;91:1985-94.
28. Pochrząst M, Basiaga M, Marciniak J, et al. Biomechanical analysis of limited-contact plate used for osteosynthesis. Acta Bioeng Biomech 2014;16:99-105.
29. Ahmad M, Nanda R, Bajwa AS, et al. Biomechanical testing of the locking compression plate: when does the distance between bone and implant significantly reduce construct stability? Injury 2007;38:358-64.
30. Nakamura R, Komatsu N, Fujita K, et al. Anteromedial plating without filling the gap in open wedge high tibial osteotomy may increase the risk of screw breakage, which can be reduced by medial plating and bone-substitute insertion. J Orthop Sci 2022. [Epub ahead of print]. doi: 10.1016/j.jos.2021.12.017.
31. Dobbe JG, Vroemen JC, Strackee SD, et al. Patient-specific distal radius locking plate for fixation and accurate 3D positioning in corrective osteotomy. Strategies Trauma Limb Reconstr 2014;9:179-83.

(English Language Editors: L. Huleatt and J. Gray)

Cite this article as: Wang X, Zhang R, Zheng X, Yu Y, Xu J, Kang Q. Geometrical analysis of the opening gap after tibial condylar valgus osteotomy for proper hinge point selection. Ann Transl Med 2022;10(23):1267. doi: 10.21037/atm-22-2022

Supplementary

Appendix 1 MATLAB code for the mathematical formulation of the opening angle with different hinge positions

1. MATLAB code

```
% Create bars with different k and MA.
clc;clear all
syms Xp Yp Xd k x y
assume(Xp>0)
assume(Yp>0)
assume(Xd>0)
assume(k>0)
r = sqrt((Xp-Xd)^2+(Yp-0)^2);
l = k*x;
equ = (l == (sqrt(r^2 - (x-Xp)^2)+Yp));
solution = solve(equ, x);
x = solution(1);
y = k*x;
bc = sqrt((x-Xd)^2 + (y-0)^2);
ab = sqrt((Xp-Xd)^2 + (Yp-0)^2);
ac = sqrt((x-Xp)^2 + (y-Yp)^2);
alpha = acos((ab^2 + ac^2 -bc^2)/(2*ab*ac));

num_row = 2;
num_column = 5;
num_pts = 3;
dist_PD = [0.625, 0.425, 0.225];
interval_k = tand(linspace(5,35,10));
color = cell(1, 3);
color{1} = [1, 0, 0]; % red
color{2} = [1, 0.7, 0];% yellow
color{3} = [0, 0.6, 0];% green
legend_pts = cell(1,3);
legend_pts{1} = 'A';
legend_pts{2} = 'B';
legend_pts{3} = 'C';

alpha_sub = cell(1,3); %The formula of 3 pts.
alpha_sub_simple = cell(1,3);
for i = 1 : num_pts
    alpha_sub{i} = subs(alpha, Yp, 0.05);
    alpha_sub{i} = subs(alpha_sub{i}, Xd, Xp + dist_PD(i));
    alpha_sub{i} = alpha_sub{i}*180/pi;
    alpha_sub_simple{i} = simplify(alpha_sub{i});

end
```


https://dx.doi.org/10.21037/atm-22-2022

```
for j = 1:length(interval_k)
    alpha_sub_value = alpha_sub_simple;
    for m = 1: num_pts
        alpha_sub_value{m} = subs(alpha_sub_simple{m}, k, interval_k(j));
        subplot(num_row, num_column, j);
        hold on
        fplot(alpha_sub_value{m}, [0.1 + 0.2 * (m - 1), 0.375 + 0.2 * (m - 1)], 'Color', color{m})
        legend(legend_pts, 'Location', 'northwest');
        legend('boxoff');
    end

    xlabel('Xp');
    ylabel('Angle');
    title([ ' Angle=' , num2str(atan(interval_k(j))*180/pi)]);

end
```

 https://dx.doi.org/10.21037/atm-22-2022